hydrology

MDPI

Article

Prioritization of Hydrological Restoration Areas Using AHP and GIS in Dulcepamba River Basin in Bolivar–Ecuador

Eddy Fernando Sanchez and Cesar Ivan Alvarez *

Environmental Research Group for Sustainable Development (GIADES), Salesian Polytechnic University, Rumichaca y Moran Valverde, Quito 170702, Ecuador; efsanchez@puce.edu.ec
* Correspondence: calvarezm@ups.edu.ec

Abstract: In this study, we performed a preliminary soil analysis and collected environmental data for the Dulcepamba River Basin in Bolivar–Ecuador, before carrying out its hydrological restoration (HR). A geographic information system (GIS) and the multicriterion Analytical Hierarchy Process (AHP) decision-making method were used. The comprehensive evaluation included morphological aspects, soil properties, climatic conditions, vegetation, and land use. The terrain conditions were investigated using indicators such as the flow capacity, topographic moisture, soil resistance, sediment transport, current density, curve number, NDVI, precipitation, and distance to rivers. The results and analysis are presented in a series of maps, which establish a starting point for the HR of the Dulcepamba watershed. The key factors for assessing soil degradation in the watershed include land use, vegetation cover, sedimentation, humidity, and precipitation. Of the studied territory, 10.7 do not require HR, while 20.28% demand HR in the long term. In addition, 30.67% require HR in the short term, and 33.35% require HR immediately. Based on the findings, it is suggested that authorities consider the environmental remediation of the watershed and propose various HR measures. This analytical approach could prove valuable as a tool for the environmental restoration of watersheds in Ecuador.

Keywords: hydrological restoration; analytical hierarchy process; GIS; soil degradation

Citation: Sanchez, E.F.; Alvarez, C.I. Prioritization of Hydrological Restoration Areas Using AHP and GIS in Dulcepamba River Basin in Bolivar–Ecuador. *Hydrology* **2024**, *11*, 81. https://doi.org/10.3390/hydrology11060081

Academic Editor: Andrea Petroselli

Received: 19 April 2024
Revised: 18 May 2024
Accepted: 21 May 2024
Published: 12 June 2024

1. Introduction

HR is defined as the restoration of river systems adversely affected by either human activities or natural occurrences. This involves leveraging historical data on precipitation, temperature, extreme flows, and vegetation cover. The overarching goal is to mitigate the impacts of intensive agriculture, erosion resulting from natural processes, biodiversity loss, and poverty, as well as to address the challenges posed by droughts and floods due to climate change. This is accomplished through the application of morphological analysis, remote-sensing techniques, GIS, and the Analytic Hierarchy Process (AHP). This study's significance is underscored by its adept integration of numerous variables, its capacity to incorporate the perceptions and preferences of diverse stakeholders into future HR decision-making processes, and its flexibility in adapting to fluctuations in data availability and shifts in watershed conditions [1–4].

By implementing the AHP in HR, this research not only provides a robust decision-making framework but also contributes to the scientific literature by providing a practical example of how advanced decision-making techniques can be applied in natural resource management. This may inspire further studies and the adoption of similar methodologies in other disciplines or in other environmental contexts, increasing the relevance and impact of the research. The method proposed in this research proposes the use of the scarce environmental data in developing countries and their HR by adjusting the model for the future with the interested parties (states, NGOs, and local communities). Unlike other HR studies, this research integrates seven morphometric variables (the SPI, TWI, TRI, STI, SD,

CN, and RD); two soil texture–vegetation cover variables (the CN and NDVI), and one climatological variable (RF). The hypothesis of this study was as follows: The integration of the GIS and AHP allows for an effective and accurate prioritization of areas requiring HR in the Dulcepamba River watershed. Areas with high soil erosion, low soil moisture, and high runoff demand immediate hydrological restoration interventions.

Hydromorphological assessment methods are essential tools for gaining an in-depth understanding to guide the most appropriate solutions for future restoration projects. The careful management of water resources is a fundamental pillar for ensuring the sustainability of river landscapes and guaranteeing a continuous supply of quality water [5]. In recent decades, agricultural intensification has resulted in significant soil degradation [6]. For territorial development planning in the Dulcepamba watershed, it is imperative to investigate HR areas capable of improving both the ecological environment and quality of life of local residents [7]. Approximately 19,000 inhabitants depend directly on agriculture and livestock; 20% live in the urban area in 20 villages [8].

The Analytic Hierarchy Process (AHP) emerges as a multicriterion decision analysis approach within the field of geographic information systems (GISs) [9–11]. In this context, two approaches to the application of the AHP are distinguished. First, it can be used to determine the weights associated with the layers of the attribute map, which can then be combined in a manner analogous to that of other weighted aggregation methods. This method is particularly useful when the number of alternatives is considerable and it is impractical to compare them. Second, the AHP principle can be used to assign priorities at all levels of the hierarchical structure, including the level representing the alternatives. In specific situations, a relatively small number of alternatives are assessed [12]. The AHP approach is predominantly used to integrate independent factors to evaluate the soil suitability for irrigation, cultivation, and groundwater recharge [13–15]. In addition, this study introduces a new perspective on the AHP based on matrices and the weighted linear combination method, relating to soil erosion hazards and the current climatic conditions, to identify and evaluate ecologically viable agricultural systems [16].

The report of the Intergovernmental Panel on Climate Change (IPCC) defines land degradation as an adverse trend caused by human activity, manifesting itself as the long-term loss of biological productivity, ecological integrity, and value to society. The United Nations Convention on Combat Desertification (UNCCD), adopted by 195 countries in 1994, recognized this problem as one of the most pressing environmental challenges [15,17,18]. Table 1 shows the soil loss in technologically intensive agricultural fields, which is 18–21 tons/ha/year, in contrast to that in fields tilled by hand, which is 0.8 tons/ha/year. Soil formation in areas without erosion is limited to only 0.05 tons/ha/year. Soil conservation techniques reduce the soil loss to between 0.004 and 0.05 tons per hectare per year, especially in stable forest ecosystems where vegetation protects the soil from erosion [19]. A total of 26% of the Dulcepamba Basin territory is short-cycle crops cultivated by hand; there is no evidence of technologically intensive agricultural methods [20].

Table 1. Soil formation and loss studies around the world.

Method	Soil Formation without Erosion	Soil Loss in Agricultural Fields	Soil Loss in Ploughed Fields	Reference
	Tn/ha/Year	Tn/ha/Year	Tn/ha/Year	
1673 measurements, 201 items	0.05	18	0.8	[21]
Megastudy, 4000 sites		21		[22]

The urgent need to evaluate HR zones will translate into concrete actions by the Autonomous Decentralized Governments of Chillanes and San Miguel, who will have to implement measures to mitigate the hydrological vulnerability in the Dulcepamba River Basin.

2. Materials and Methods

2.1. Location

In Figure 1, we observe the spatial extent of the Dulcepamba River Basin, an area of significant interest in the realm of HR, nestled within the Chillanes and San Miguel cantons of Bolivar Province, Ecuador. Covering an expansive 395 square kilometers, this basin represents a crucial ecosystem for restoration efforts. Notably, the hydrological dynamics of the region exhibit distinct seasonal patterns, with precipitation peaking from December to May, averaging between 93 and 257 mm per month. Conversely, the dry season from June to November witnesses a stark reduction in rainfall, with averages ranging from 9 to 31 mm per month [23]. Understanding these precipitation trends is paramount for effective restoration strategies.

Furthermore, the thermal regimes within the basin exhibit variability across its topographical gradients. In San Pablo de Atenas, temperatures range from 11 to 21 degrees Celsius, while in San Pablo de Amalí, they span from 20 to 27 degrees Celsius [24]. These temperature differentials influence ecological processes, including vegetation growth and water availability, thereby emphasizing the importance of comprehensive hydrological management in restoration endeavors within the Dulcepamba Basin.

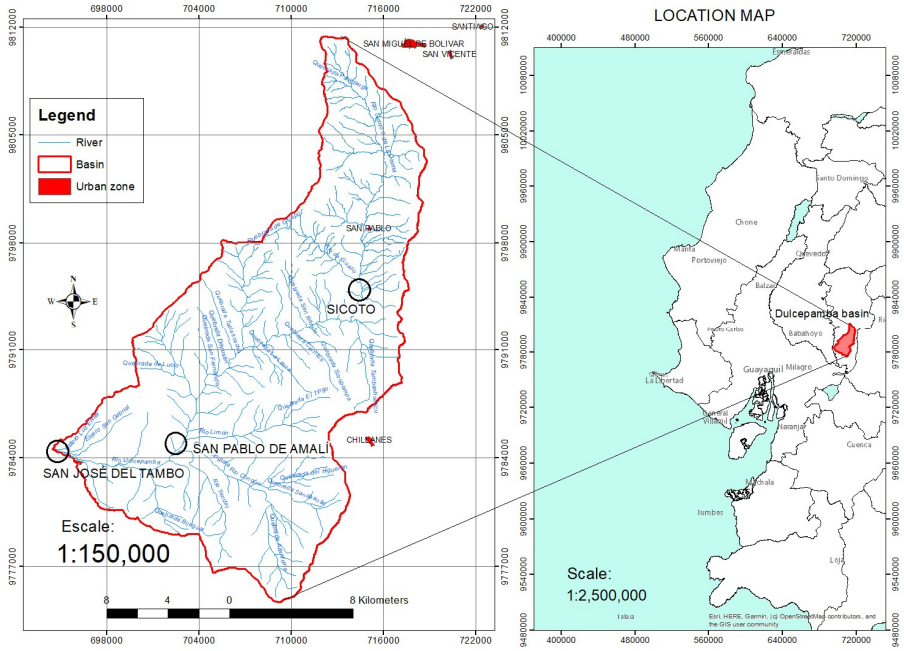

Figure 1. Dulcepamba River catchment area (coordinate system: Datum WGS 84—Projection UTM Zone 17 S) [25].

2.1.1. Average Flow and Hydrological Variability

The monthly flow averages at San Pablo and Amalí are presented in Table 2. The observed flow at Sicoto of 26.94 cms in March 1983 modeled peak floods of 84.5 cms, with a continuous flow of 40 cms in 10 days (return interval—25 years), similar to February 2008. The observed flow at Sicoto of 19.2 cms in March 2015 modeled a peak flood of 60 cms (return interval—5 years) (see Table 3). The climatic anomalies in the study area are reflected in the extreme flow increases in the Dulcepamba River in the Sicoto and San Pablo de Amalí sectors [26].

Table 2. Monthly flow averages at San Pablo de Amalí [26].

Monthly Flow Averages at Amalí (cms)											
Jan.	**Feb.**	**Mar.**	**Apr.**	**May**	**Jun.**	**Jul.**	**Aug.**	**Sep.**	**Oct.**	**Nov.**	**Dec.**
7.51	10.6	12.13	12.85	8.69	4.91	3.21	2.71	2.82	3.08	3.42	4.42

Table 3. Exceedance flows at San Pablo de Amalí [26].

Month	Year	Observed Flow		Hydrologic Model (cms)		
		Sicoto	San José del Tambo	San Pablo de Amalí		
		Peak (cms)		Peak (cms)	Continuous (cms)	Time (day)
Apr.	1970	7.4	31.7			
Mar.	1983	26.9		84.5 *	40.0	10.0
Mar.	1989	12.5				
Jan.	1993	3.0				
Feb.	2008	25.8		86.1 *	50.0	15.0
Mar.	2015	19.2		60 **		

* 25-year return interval; ** 5-year return interval.

2.1.2. Different Land Uses in the Dulcepamba Basin

Table 4 shows the vegetation cover of the Dulcepamba watershed, with 49.3% planted pasture, 26.1% short-cycle crops, 9.1% natural forest, 8.4% perennial crops, and 7.1% shrub vegetation [20]. Urbanization and infrastructure in 2014 were marginal, equivalent to 1332 ha (0.33%) of the entire province of Bolivar [8].

Table 4. Vegetation cover in the Dulcepamba Basin [20].

Vegetation Cover	%
Planted grasses	49.3
Short-cycle crops	26.1
Natural forest	8.0
Shrub vegetation	7.1
Sugar cane	4.5
Coffee–cocoa	3.7
Intervened natural forest	1.1
Undifferentiated crops	0.2
Corn	0.1
TOTAL	100.0

2.1.3. Poverty in the Dulcepamba Basin

By utilizing unsatisfied basic needs (UBNs) as a measure of poverty, it becomes evident that in the cantons of San Miguel and Chillanes, home to the Dulcepamba watershed, the UBN rate stands at 76.3%, in contrast to the national average of 69.3% [8] (see Table 5).

Table 5. Poverty in the Dulcepamba Basin [8].

Poverty Due to Unmet Basic Needs (UBNs) (%)				
Canton	Women in households with inadequate services	Men in households with inadequate services	Women in households with economic dependence	Men in households with economic dependence
San Miguel	69.6	70.1	8.1	7.8
Chillanes	80.9	80.7	9.6	10.3

2.2. Basic Data

In the field of digital cartography, a detailed map at a scale of 1:50,000 has been meticulously prepared that outlines the topography of San Miguel de Bolívar, Chillanes, and Matilde Esther, taking advantage of the data sets housed in the Geoportal of the Military Geographic Institute from Ecuador [25]. This mapping effort has been enhanced by the generation of a digital elevation model (DEM) that has a resolution of 10 m per pixel, as illustrated in Figure 2.

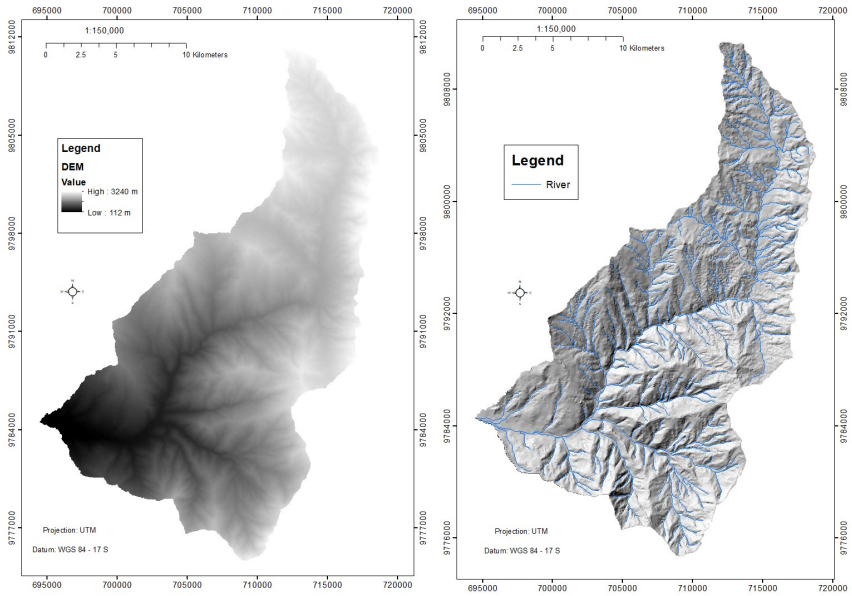

Figure 2. Digital elevation model (DEM) (10 m pixel) and topographic relief.

To complement this mapping, Sentinel-2 satellite images covering the time window from 17 April 2018 to 30 August 2019 [27] have been leveraged, along with relevant data related to texture and vegetation cover from the year 2017 [20].

2.3. Criteria and Spatial Variables for HR in the Research Region

In this study, several variables that influence hydrology were considered to identify areas where HR is likely to be required. These variables included the following:

SPI	Stream Power Index;
TWI	Topographic Wetness Index;
TRI	Terrain Ruggedness Index;
STI	Sediment Transport Index;
SD	Stream Density Index;
CN	Curve Number Index;
RD	Distance from River;
NDVI	Normalized Difference Vegetation Index;
RF	Rainfall Index.

a. SPI—Stream Power Index

The SPI, or Stream Power Index, is a measure that evaluates the ability of a stream to transport sediment. Negative SPI values indicate areas prone to sediment accumulation, whereas positive values indicate areas with steep slopes and an increased risk of erosion. This index specifically quantifies the erosive power of the surface flow [28]. In the process of calculating the SPI, we employed a digital elevation model (DEM) of the watershed, along with ArcGIS tools such as Flow Direction, Flow Accumulation, and Slope. In addition, we applied Equation (1):

$$\text{SPI} = Ln((\text{Flow Accumulation} + 0.001) * (\tan\,(Slope_{radians}) + 0.001)) \quad (1)$$

b. TWI—Topographic Wetness Index

The TWI is an index that reflects the propensity of an area to retain water [29]. To calculate the TWI, we employed the digital elevation model (DEM) of the watershed along with SagaGis tools, which included Fill Sinks, Flow Accumulation (top-down), Specific Catchment Area (SCA), β: slope (radians), and Equation (2):

$$\text{TWI} = \log_e \frac{SCA}{\tan \beta} \tag{2}$$

c. TRI—Topographic Roughness Index

The TRI, or Terrain Robustness Index, is an objective quantitative metric that assesses the topographic heterogeneity by calculating the total elevation change between a grid cell and its eight neighboring cells in a digital elevation model (DEM). This index is important for predicting the habitats preferred by species and the density at which they are located in various environments and is often an essential component of the niche of such species [30]. In the process of calculating the TRI, the DEM of the basin was used, as well as the Focal Statistics tool of ArcGIS [31] and Equation (3):

$$\text{TRI} = \frac{(Smooth\ Roughness - Minimum\ Roughness)}{(Maximun\ Roughness - Minimum\ Roughness)} \tag{3}$$

d. STI—Sediment Transport Index

The STI, or Sediment Transport Index, is a crucial tool for obtaining essential information about the sediment movement in a given basin, and its calculation is based on Equation (4) [32]:

$$\text{STI} = \left(\frac{As}{22.13}\right)^{0.6} * \left(\frac{\sin \beta}{0.0896}\right)^{1.3} \tag{4}$$

where, As is the Flow Accumulation and β is the slope (percent rise);

e. SD—Stream Density Index

The stream density (SD) is a key indicator of the water supply potential in a watershed and is able to characterize aspects such as the erosion, permeability, slope, and vegetation cover in that area [33]. For its calculation, the Line Density tool of ArcGIS was used together with Equation (5):

$$\text{SD} = \sum \left(\frac{Stream\ lenght}{Study\ area}\right) \tag{5}$$

f. CN—Curve Number Index

The curve number (CN) is an indicator related to the amount of runoff and depends on several factors, such as the soil type, vegetation cover, and slope of the terrain [33] (p. 188);

g. RD—River Distance Index

The RD, which represents the longitudinal distance to the river axis, is closely related to peak flows in winter and has the potential to induce erosion and mass movements in soils adjacent to the river;

h. NDVI—Normalized Difference Vegetation Index

Equation (6) and a combination of Sentinel-2 images from 17 April 2018 and 30 August 2019 were used to calculate the NDVI [27]:

$$\text{NDVI} = \frac{(NIR - R)}{(NIR + R)} \tag{6}$$

The NIR (near-infrared) and R (red) values represent the reflectance obtained from multispectral satellite images. Healthy vegetation, owing to the presence of chlorophyll,

exhibits a low albedo. The Normalized Difference Vegetation Index (NDVI) ranges from 0.1 to 1, and values close to 1 indicate an optimal state of health for vegetation [34];

i. RF—Rainfall Index

The RF variable corresponds to the monthly precipitation expressed in millimeters in the region of interest, as shown in Figure 3 [23].

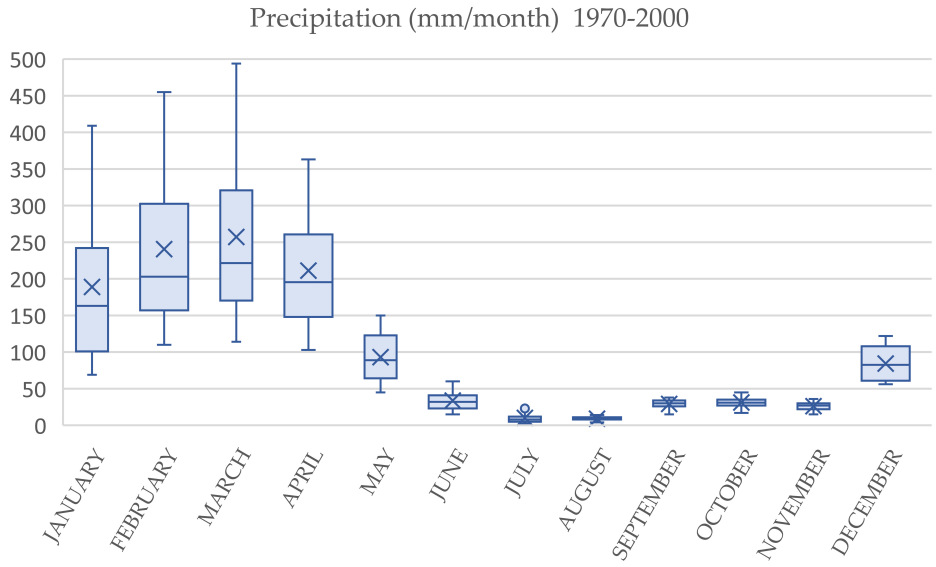

Figure 3. Monthly rainfall in the Dulcepamba Basin.

2.4. Assessment and Categorization of Variables

Table 6 shows the principles based on which weights are assigned to the different HR variables of the hydrological basin.

Table 6. Principles for assigning weights in the river basin.

Index	Values	Principles for Assigning Weightings
SPI	Negative Positive	Potential deposition areas Potential erosive areas
TWI	Low High	Accumulates water Does not accumulate water
TRI	Low Medium High	Level ground surface Intermediate rough surface Extremely rough surface
STI	Low High	Less sediment transport Greater sediment transport
SD	Low High	Soils very resistant to erosion Soils easily eroded
NC	Low High	Permeable soils Impermeable soils
RD	Short Long	Erosion and mass movement × runoff Erosion and low mass movement × runoff
NDVI	0.62–0.94 <0.51	Healthy vegetation Stressed vegetation
RF	290–478 114–224	High rainfall Low rainfall

Table 7 presents the nine HR evaluation criteria in detail, along with their respective categories and assigned weightings. To determine the levels and classify the information content according to the definition of the indicator, we used the Jenks Natural Breaks classification, as proposed in [35].

Table 7. Assessment and categorization of variables.

Canon	Weight	From	To	Area (395 km^2: 100%)	Category
SPI	1	−13.8	−10.1	2.5	High sediment accumulation
	2	−10.1	−3.9	10.1	Smooth accumulation of sediment
	3	−3.9	0.5	25.4	Medium sediment accumulation
	4	0.5	3.0	51.1	Medium erosion
	5	3.0	14.4	10.9	Heavy erosion and soil degradation
TWI	1	13.8	25.3	1.1	Flooding
	2	8.2	13.8	12.1	Heavy accumulation of water
	3	5.5	8.2	44.9	Medium water accumulation
	4	4.2	5.5	35.6	Low water accumulation
	5	1.4	4.2	6.4	Very low water accumulation
TRI	1	0.0	1.1	12.9	Level ground surface
	2	1.1	2.7	31.1	Slightly rough surface
	3	2.7	4.1	33.0	Moderately rough surface
	4	4.1	6.1	18.4	Very hilly surface
	5	6.1	18.3	4.6	Extremely rugged surface
STI	1	0.0	119.7	98.7	No sediment transport
	2	119.7	127.4	0.1	Little sediment transport
	3	127.4	247.1	0.5	Very little sediment transport
	4	247.1	2106.8	0.6	Some sediment transport
	5	2106.8	31,004.4	0.1	Increased sediment transport
SD	1	0.2	1.9	15.6	Highly permeable and erosion-resistant soils
	2	1.9	2.8	28.6	Moderately permeable soils
	3	2.8	3.7	30.5	Poorly permeable soils
	4	3.7	4.8	20.0	Moderately impermeable soils
	5	4.8	8.1	5.3	Impermeable soils, sparse vegetation cover
CN	1	36.0	59.1	6.1	Soils with very low runoff
	2	59.1	71.4	26.2	Low-runoff soils
	3	71.4	78.0	31.2	Soils with medium runoff
	4	78.0	81.4	15.5	Soils with intermediate runoff
	5	81.4	88.0	21.1	High-runoff soils
RD	1	100.0	4000.0	74.4	Very low erosion and mass movement due to runoff
	2	60.0	100.0	11.8	Erosion and low mass movement due to runoff
	3	30.0	60.0	6.8	Less erosion and mass movement due to runoff
	4	15.0	30.0	3.2	Moderate erosion and mass movement due to runoff
	5	0.0	15.0	3.8	Potential erosion and mass movement due to runoff
NDVI	1	0.7	0.9	28.6	Healthy vegetation
	2	0.6	0.7	29.6	Moderately healthy vegetation
	3	0.5	0.6	23.9	Low-stress vegetation
	4	0.4	0.5	13.7	Moderately stressed vegetation
	5	−0.1	0.4	4.1	Highly stressed vegetation
RF	1	380.0	478.0	6.7	High rainfall (mm)
	2	291.0	380.0	13.5	Average high rainfall (mm)
	3	224.0	291.0	19.9	Average rainfall (mm)
	4	169.0	224.0	31.7	Low average rainfall (mm)
	5	114.0	169.0	28.2	Low rainfall (mm)

2.5. Weighting of Factors Influencing the HR of the Dulcepamba Watershed

The Analytical Hierarchical Process (AHP) is a fundamental analytical method for addressing complex hydrological decisions. This approach involves weighting the variables that delineate the phenomenon under study, using a pairwise comparison matrix to derive a scale of importance and the associated weights (see Figure 4).

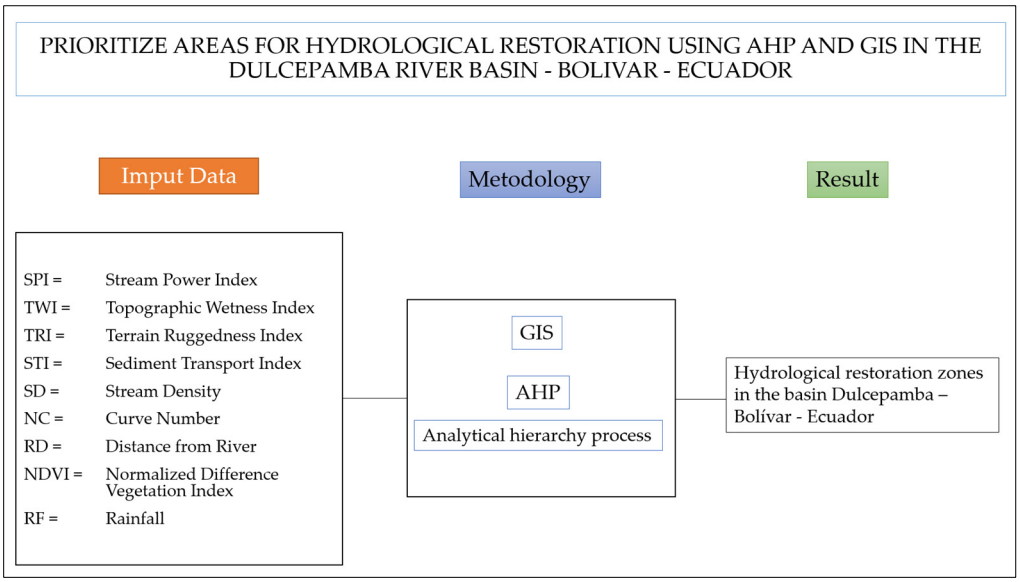

Figure 4. Data entry, methodology, and results of the survey.

The AHP, initially proposed in [36], is a semi-objective, multi-objective, and multicriterion method. This multicriterion decision-making approach favors the choice of preferences among several alternatives using single scales [36]. Its application is widely recognized in the environmental susceptibility research, decision making, and regional planning [34,37] (refer to Table 8).

Table 8. Nine-point analytical hierarchy scale [38].

Degree of Importance	Definition	Interpretation
1	Equal importance	Two activities contribute equally to the objective
3	Moderate importance	Experience and judgment slightly favor one activity over the other
5	Strong importance	Experience and judgment strongly favor one activity over the other
7	Very strong or demonstrated	One activity is much more favored than the other; its dominance has been demonstrated in practice
9	Extreme	Evidence strongly favors one activity over the other; it is absolute and completely clear
Scales 2, 4, 6, and 8	Intermediate values	A compromise between adjacent values is needed
Reciprocal	aij = 1/aji	Hypothesis of the method

The AHP involves several steps. In the initial phase, unstructured problems and the research objectives are defined. The variables that affect the problem are then identified and organized in a hierarchy (those with higher relative weights are considered more important relative to the others) [34]. Subsequently, rank values are assigned to assess the relative importance of each factor, according to their subjective significance (T. L. Saaty & Vargas, 2012, 2013; T. Saaty & Vargas, 2006) [39–41]. In the context of the variables detailed in Table 7, any aspect linked to environmental sensitivity is interconnected and can be evaluated in a mutually relevant manner using the pairwise comparison technique of the AHP [42].

3. Results

3.1. Spatialization of Evaluated Parameters

Upon reviewing the maps presented in Figure 5, the following observations can be made: SPI: 62% of the territory shows signs of erosion; TWI: 13% of the territory exhibits areas with significant water accumulation; TRI: 44% of the territory displays a surface that ranges from level to slightly rough, while 23% has a very rough surface; STI: the sediment transport in the basin is minimal; SD: 44% of the soils demonstrate generally high permeability; CN: 33% of the soils have low runoff, while 37% experience from intermediate to high runoff; RD: 4% of the territory is susceptible to fluvial erosion and mass movements due to increased river flows; NDVI: 42% of the vegetation shows signs of varying degrees of stress; RF: 28% of the territory in the upper watershed zone receives lower rainfall compared to other areas.

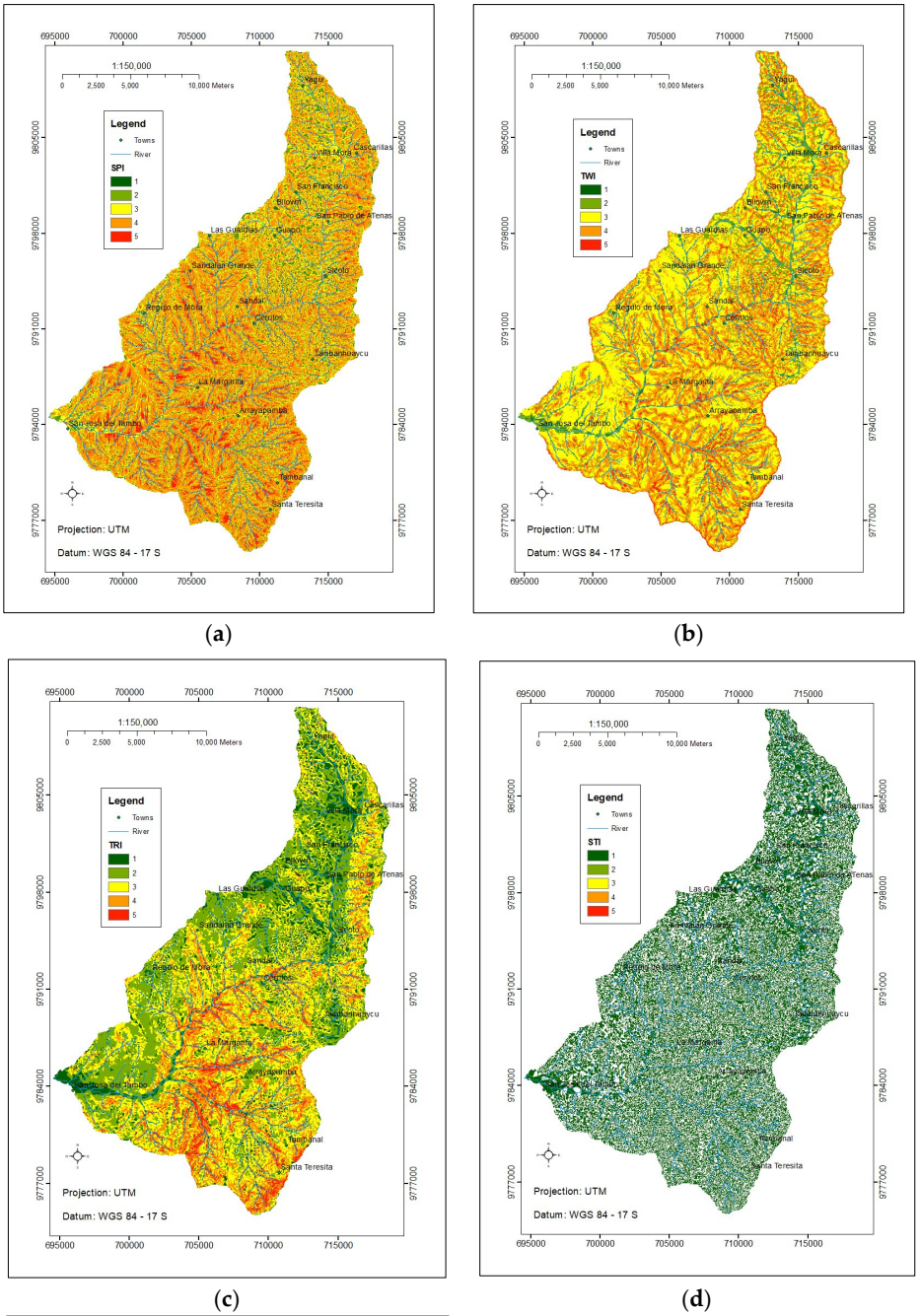

Figure 5. *Cont.*

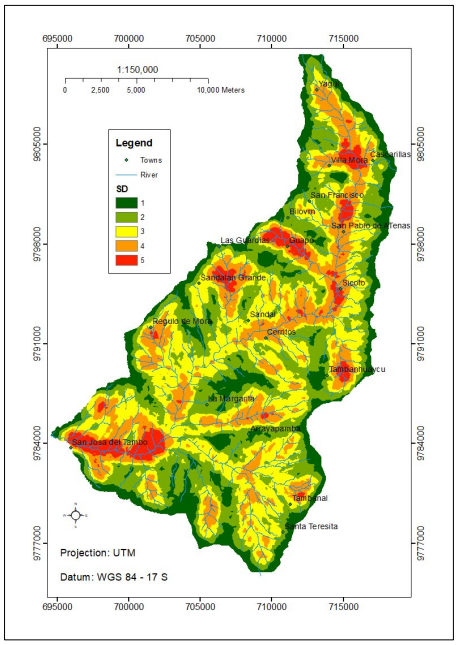

(**e**)

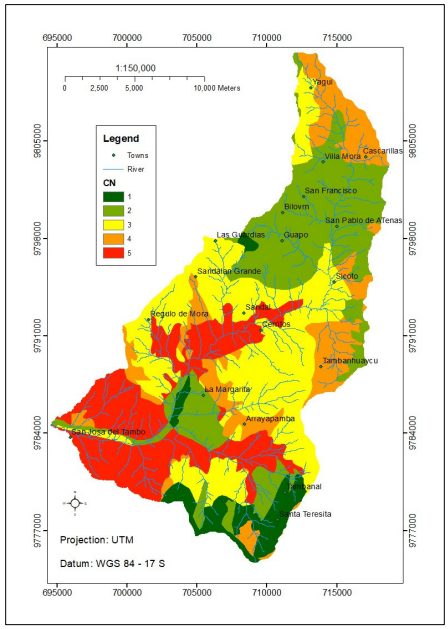

(**f**)

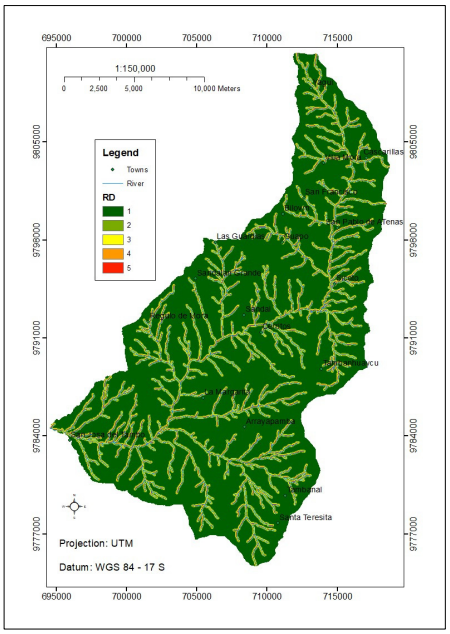

(**g**)

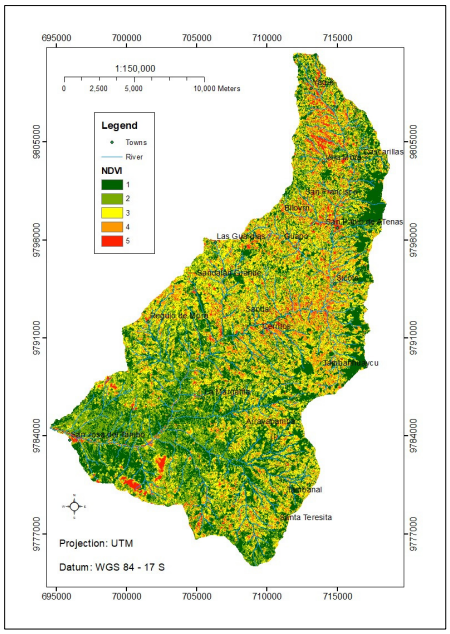

(**h**)

Figure 5. *Cont*.

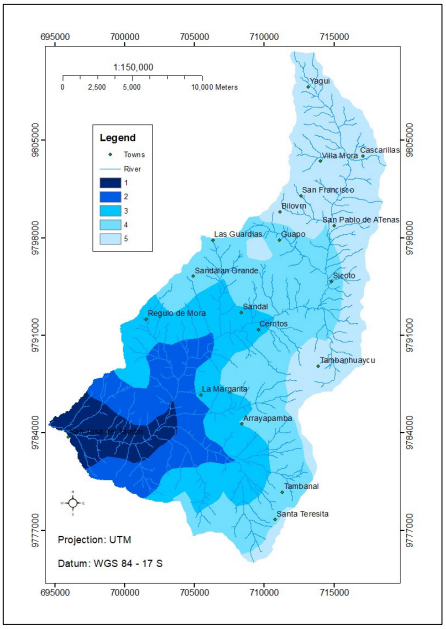

(**i**)

Figure 5. Maps: (**a**) Stream Power Index; (**b**) Topographic Wetness Index; (**c**) Topographic Roughness Index; (**d**) Sediment Transport Index; (**e**) Stream Density Index; (**f**) Curve Number Index; (**g**) River Distance Index; (**h**) NDVI; (**i**) Rainfall Index.

3.2. Evaluation of Elements Using the AHP Method

Considering the results obtained by the AHP method in the present study, where the SPI, TWI, TRI, STI, SD, CN, RD, NDVI, and RF variables were examined, Tables 9 and 10 present the evaluations of the factor pairs and the results of the weighted variables. To derive the Consistency Index (CI), Equation (7) was applied, where "n" represents the number of factors ($n = 9$) and "λ" denotes the average value of the consistency vector, as detailed in Table 11. Thus, the CI calculation result was 0.06 [43]:

$$\mathrm{CI} = \frac{(\lambda - n)}{(n - 1)} = \frac{(9.5 - 9)}{(9 - 1)} = 0.06 \quad (7)$$

Table 9. Evaluation of the comparison between nine criteria, using the AHP method.

	SPI	TWI	TRI	STI	SD	CN	RD	NDVI	RF
SPI	1.00	0.25	2.00	1.00	1.00	0.33	0.33	0.33	1.00
TWI	4.00	1.00	3.00	4.00	3.00	1.00	3.00	1.00	1.00
TRI	0.50	0.33	1.00	0.33	0.33	0.25	0.50	0.25	0.33
STI	1.00	0.25	3.00	1.00	1.00	0.25	1.00	0.50	1.00
SD	1.00	0.33	3.00	1.00	1.00	0.50	1.00	0.33	1.00
CN	3.00	1.00	4.00	4.00	2.00	1.00	4.00	1.00	1.00
RD	3.00	0.33	2.00	1.00	1.00	0.25	1.00	1.00	1.00
NDVI	3.00	1.00	4.00	2.00	3.00	1.00	1.00	1.00	1.00
RF	1.00	1.00	3.00	1.00	1.00	1.00	1.00	1.00	1.00
Total	17.50	5.50	25.00	15.33	13.33	5.58	12.83	6.42	8.33

Table 10. Determination of relative criterion weights.

	SPI	TWI	TRI	STI	SD	CN	RD	NDVI	RF	RESULT	%
SPI	0.06	0.05	0.08	0.07	0.08	0.06	0.03	0.05	0.12	0.06	6.45
TWI	0.23	0.18	0.12	0.26	0.23	0.18	0.23	0.16	0.12	0.19	18.94
TRI	0.03	0.06	0.04	0.02	0.03	0.04	0.04	0.04	0.04	0.04	3.76
STI	0.06	0.05	0.12	0.07	0.08	0.04	0.08	0.08	0.12	0.08	7.59
SD	0.06	0.06	0.12	0.07	0.08	0.09	0.08	0.05	0.12	0.08	7.97
CN	0.17	0.18	0.16	0.26	0.15	0.18	0.31	0.16	0.12	0.19	18.79
RD	0.17	0.06	0.08	0.07	0.08	0.04	0.08	0.16	0.12	0.09	9.45
NDVI	0.17	0.18	0.16	0.13	0.23	0.18	0.08	0.16	0.12	0.16	15.57
RF	0.06	0.18	0.12	0.07	0.08	0.18	0.08	0.16	0.12	0.11	11.47
										1.00	100.00

Table 11. Consistency Index (CI) and Consistency Range (CR).

M = NW	QUOTIENT = M/W	CI = ($\lambda - n$)/($n - 1$)	0.06
0.60	9.36	$CR = CI/RI$	0.04
1.85	9.74		
0.36	9.47		
0.71	9.41		
0.75	9.42		
1.83	9.76		
0.90	9.51		
1.48	9.49		
1.08	9.38		
λ=	9.50		
n=	9.00		

To determine the Consistency Radius (CR), Equation (8) was used [43], where "RI" is the Random Inconsistency Index, dependent on the number (n) of factors under comparison; for n = 9, RI = 1.45, as indicated in Table 12 [36,43]. The CR is calculated as follows:

$$CR = \frac{CI}{RI} = \frac{0.06}{1.45} = 0.04 \quad (8)$$

Table 12. Random Index (RI) values [44].

n	1	2	3	4	5	6	7	8	9	10	11	12	13	14	15
RI	0.00	0.00	0.58	0.90	1.12	1.24	1.32	1.41	1.45	1.49	1.51	1.53	1.56	1.59	1.67

Following the recommendation in [45], when the CR is less than 0.1, it indicates a realistic degree of consistency in the pairwise comparison. Consequently, according to the results (Figure 6), the weights 6.45%, 18.94%, 3.76%, 7.59%, 7.97%, 18.79%, 9.45%, 15.57%, and 11.47% are assigned to the SPI, TWI, TRI, STI, SD, CN, RD, NDVI, and RF categories, respectively [43]. The combination of different factors in the nine selected maps, using GIS tools, revealed that the TWI, CN, NDVI, and RF variables contributed 64.77% to the total HR parameters in the Dulcepamba watershed.

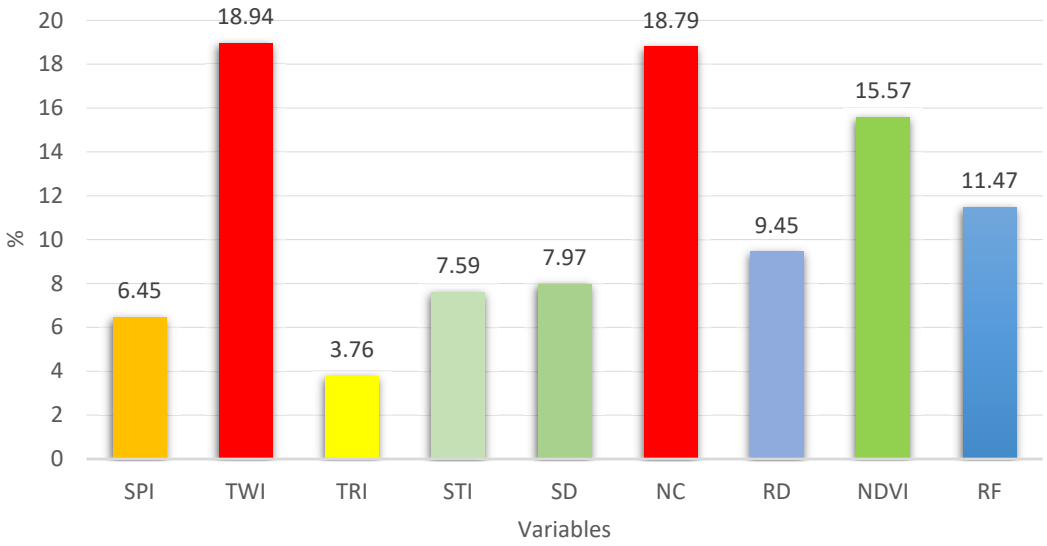

Figure 6. Overall contributions of HR parameters.

3.3. Prioritization of Areas of HR

With the following percentages assigned to the respective variables: SPI (6.45%); TWI (18.94%); TRI (3.76%); STI (7.59%); SD (7.97%); CN (18.79%); RD (9.45%); NDVI (15.57%); and RF (11.47%), the Raster Calculator and Reclassify tools of ArcGIS were used to obtain the HR areas in the Dulcepamba River watershed. The results are presented in Table 13. For cartographic representation, the map was classified into five categories (low, low–medium, medium, high, and very high) using the Natural Breaks Jenks method [46–48].

Table 13. HR priority.

Weight	From	To	Category
1	122.93	236.24	Low HR
2	236.24	265.93	Low–medium HR
3	265.93	292.28	Average HR
4	292.28	322.17	High HR
5	322.17	461.64	Very high HR

The resulting map, with a resolution of 10 m per pixel, is shown in Figure 7. Table 14 shows the area and percentage corresponding to each HR category.

Table 14. Areas and percentages of HR in the Dulcepamba River Basin.

HR	Area (km^2)	%
Low	42.29	10.70
Low–Medium	99.90	25.28
Medium	121.21	30.67
High	93.13	23.56
Very High	38.70	9.79
Total	395.23	100.00

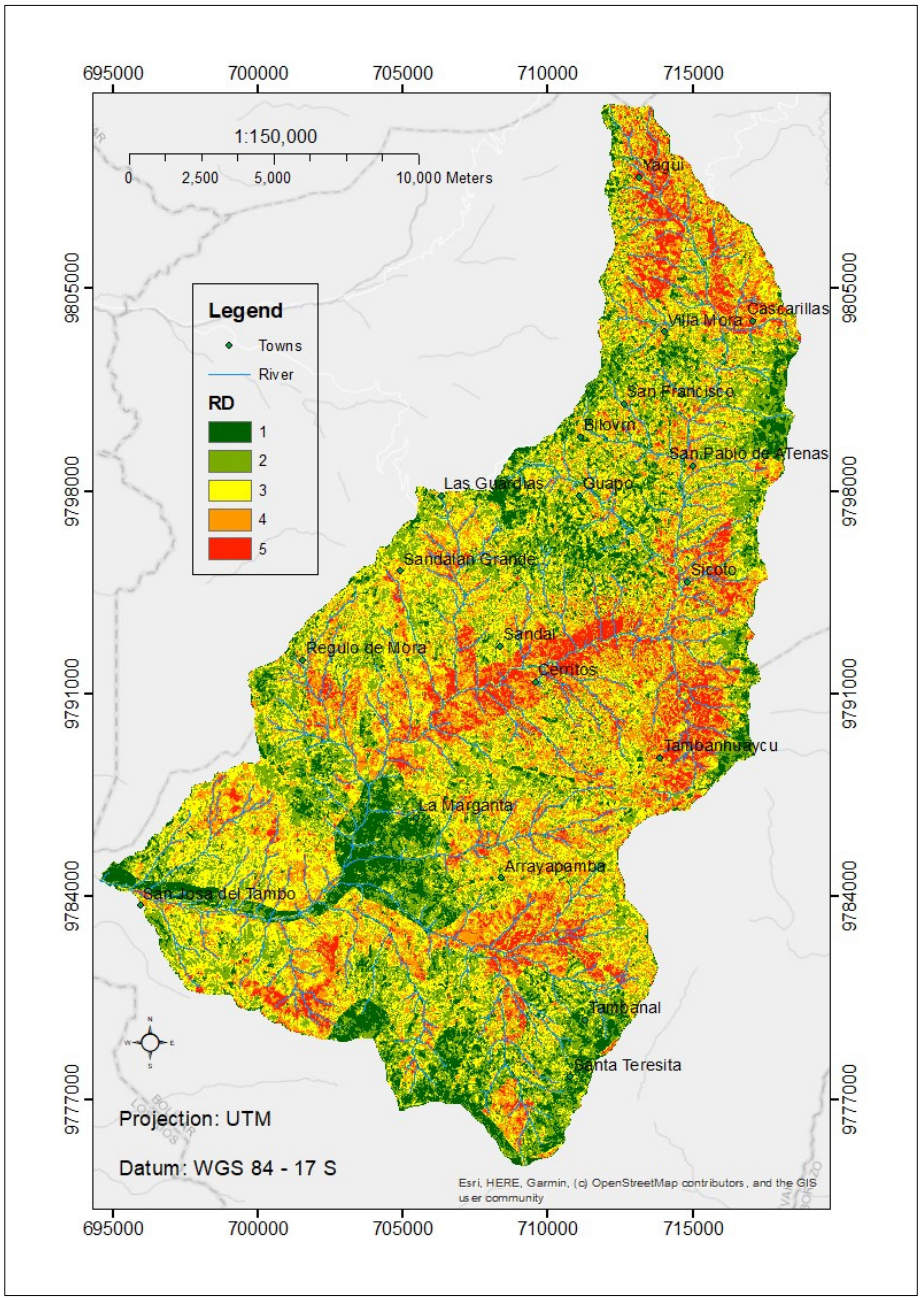

Figure 7. Prioritized HR areas from 1 to 5 (from low to very high).

4. Discussion

The following is a discussion of the values of the variables analyzed in the maps in Figure 5: SPI: Most of the territory is experiencing soil loss, which negatively affects the soil productivity. TWI: The territory is prone to low-humidity conditions, which benefit the erosion risk but limit the water availability to plants. TRI: Areas with higher roughness may be more prone to erosion and mass movement. STI: This index indicates that there is little sediment movement in the watershed, indicating that it is positive for the water quality. SD: Soils with high permeability allow good water infiltration, which reduces surface runoff and erosion. CN: Soils with high runoff are at a higher risk of erosion and should be managed more carefully. RD: A low percentage of susceptibility suggests that most of the territory is not at high risk of fluvial erosion, but affected areas require specific attention. NDVI: A significant proportion of vegetation is stressed, which may be indicative of problems such as lack of water, disease, or unfavorable soil conditions. RF: Areas with

lower rainfall are more vulnerable to drought and may have greater challenges in terms of water availability for restoration. The variables causing the spatial patterns in Figure 7 in order of priority are as follows: the TWI, NC, NDVI, RF, SD, STI, SPI, and TRI.

In the context of topographic indices, the control of soil erosion and sediment transport can be calculated using empirical methods or simple equations, as highlighted in previous studies [49]. These indices have demonstrated accurate specificity in delineating shallowly saturated zones and in determining the soil water content in our study area [50–52]. The results derived from the Topographic Wetness Index (TWI) indicate high reliability for vegetation assessment by accounting for the spatial distribution of the soil moisture, a critical factor in the formation of surface runoff [53,54]. The Soil Loss Index (SPI), which estimates the amount of erosion on a slope affected by the surface flow, has emerged as a valuable tool for identifying areas prone to sediment transport and different forms of soil erosion. Consequently, these areas highlight the suitability of afforestation as an effective measure for controlling soil erosion [49]. In the initial stages of land rehabilitation, priority should be given to local and native pioneer species as part of a sustainable development strategy for natural resource preservation [7].

To prioritize sub-watersheds according to their potential erosion risk and water availability, we integrated the morphometric parameters, precipitation, NDVI, and soil texture, based on previous investigations [51,55,56]. Topographic features play a crucial role in soil erosion and sediment transport processes by influencing the surface flow [7,57]. An analysis of the secondary topographic indices (the TWI, SPI, and STI) was performed to generate a relative susceptibility map for hydrogeomorphological restoration. The most prominent reasons for this environmental susceptibility are steep slopes and sparse vegetation cover [58].

Climate change affects agricultural production by altering the water availability, soil quality, and nutrient levels [19]. The threat of soil erosion affects agricultural productivity, ecosystem functionality, and environmental sustainability. This phenomenon leads to a reduction in organic matter and essential nutrients, such as nitrogen, phosphorus, and potassium [19]. In addition, it affects ecosystem functions and services, including soil formation, hydrological cycling, and soil nutrient cycling [59], leading to a reduction in biodiversity, water quality, and food security [60]. The identification and prioritization of critical areas can be used to implement land-use planning and development actions to mitigate the impact of soil erosion [51,61,62]. Table 15 shows that 38% of the soil on the planet is used for agriculture (1850–2011), and several studies suggest that the degraded soil on the planet has reached an average of 27% (1983–2015). According to this study, approximately 33% (130 km^2) of the Dulcepamba watershed and less than 40% of the degraded soil in Bolivar Province (4310 km^2) require high–very high restoration [8]. According to [63], agricultural productivity worldwide has decreased by 20% (1999–2013) due to soil degradation.

Table 15. Agricultural and degraded land on Earth.

Method	Years		Agricultural Land	Degraded Soil		Reference
			%	Mkm^2 ‡	% Free Ice	
--	1850	2011	38			[64,65]
NDVI, biophysical models, and a database of abandoned agricultural land		2015		10–60	8–45	[66]
NDVI	1983	2011			24	[67]
NDVI, biomass, global vegetation model	1982	2010			17–36	[68]

Table 15. *Cont.*

Method	Years		Agricultural Land	Degraded Soil		Reference
			%	Mkm² ‡	% Free Ice	
NDVI	1981	2006			29	[69]
--	2015	2020		4.31×10^{-3}	40	Bolivar Province [8]
NDVI, AHP		2024		1.3×10^{-4}	33	Current study

‡ million km².

The Analytical Hierarchy Process (AHP) multicriterion spatial assessment method for assessing land degradation has been widely used in environmental assessments [70–72]. Jain Ref. [70] found efficiency in the calculation of indices and remote-sensing techniques to investigate the relative vulnerability to soil erosion. Several researchers have attempted to assess the crop suitability, susceptibility, and hydrologic health of watersheds using AHP methods [51,71,72]. This study attempts to introduce a new AHP approach based on matrices and the linear and weighted combination method, in relation to soil erosion hazards, runoff, infiltration, and land use, to identify and evaluate ecologically viable agricultural systems [6,13–16].

The AHP effectively integrates variables into a coherent and structured framework, prioritizes restoration actions, can include stakeholder preferences, allows stakeholders to understand how and why certain decisions are made (government, NGOs, and local communities), and can be adjusted according to the data availability, which is limited in developing countries [6,73,74]. This study also contributes to the scientific literature by providing a practical example of how advanced decision-making techniques can be applied in natural resource management.

5. Conclusions and Recommendations

In the rainiest months (March–April), the most affected areas from the hydrological point of view are located in the high–very high HR zones, as shown in Figure 7. Approximately one-third of the territory of the Dulcepamba watershed exhibits considerable degradation in its hydrological conditions, reaching 33.35%. In contrast, 10.7% of the evaluated area does not require HR intervention, while 20.28% requires this type of action in the long term. In addition, 30.67% requires short-term interventions, and 33.35% requires immediate HR; thus, the hypothesis of this study is fulfilled. To address the HR, the decision makers would be as follows: the Prefecture of Bolivar Province, the Dulcepamba Project [75], and local communities.

When using the maps, the following is recommended: SPI: Reduce erosion with the intervention of the Prefecture of Bolivar and its Secretariat of Environmental Management and Natural Risks with training programs for environmental monitoring and evaluation. TWI: Construct permeable water retention structures to enhance infiltration. TRI: Prioritize biological restoration in highly rugged areas, using native species. SD: Enhance connectivity within biological ecosystems. CN: Give precedence to reforestation initiatives with native species in regions experiencing high runoff. RD: Establish riparian barriers with indigenous vegetation. NDVI: Utilize drones equipped with multispectral cameras to assess indicators following interventions in high-risk areas. RF: Develop stormwater management systems to prepare for extreme events like floods and droughts.

The professional in charge of the HR strategy must possess a deep understanding of the specific environmental conditions of the location, as well as understand the social and economic requirements of the region [76]. Achieving HR involves balancing the hydrological, ecological, and agricultural conditions using techniques such as terracing, check dams, and native afforestation [76]. Transverse ditches filled with gravel and sand can be used to effectively increase soil moisture [77]. To improve the sustainability of a watershed, it is essential to identify aspects such as the water quantity and quality, species,

ecosystems, resilience to climate change, and local culture [78,79]. Ecological management aimed at improving the quality of land use involves the transformation of grasslands into forests. The water conservation capacity (WC) of forests per square kilometer exceeds 600 mm, whereas that of grasslands is approximately 192 mm, and arid lands can result in a loss of approximately 300 mm of their WC [80].

Author Contributions: E.F.S.: investigation, conceptualization, methodology, and software. C.I.A.: review and supervision. All authors have read and agreed to the published version of the manuscript.

Funding: This research received no external funding.

Data Availability Statement: Analyzed data can be provided upon request.

Conflicts of Interest: The authors declare no conflicts of interest.

References

1. Hämmerling, M.; Kocięcka, J.; Zaborowski, S. AHP as a Useful Tool in the Assessment of the Technical Condition of Hydrotechnical Constructions. *Sustainability* **2021**, *13*, 1304. [CrossRef]
2. Cecílio, R.A.; Oliveira-Ravani, L.T.; Zanetti, S.S.; Mendes, H.A. Method for classifying sites to Atlantic Rainforest restoration aiming to increase basin's streamflows. *IForest* **2021**, *14*, 86. [CrossRef]
3. Leuschner, A.C.; Van Gasselt, S.; Merz, C. *GIS-Gestützte Analysen zur Erfassung Anthropogener Einflüsse auf den Landschaftswasserhaushalt*; Wichmann Verlag: Berlin/Heidelberg, Germany, 2017; ISBN 978-3-87907-633-8.
4. El Haj, F.A.; Ouadif, L.; Akhssas, A. Identification of soil erosion-susceptible areas using Analytical Hierarchy Process (AHP) and GIS. *J. Southwest Jiaotong Univ.* **2023**, *58*. [CrossRef]
5. Sulaiman, M.S.; Goh, Q.Y.; Sang, Y.F.; Sivakumar, B.; Ali, A.; Rasit, N.; Abood, M.M. Development of river morphologic stability index (RMSI) to assess mountain river systems. *J. Hydrol. Reg. Stud.* **2021**, *37*, 100918. [CrossRef]
6. Kumar, A.; Pramanik, M.; Chaudhary, S.; Negi, M.S. Land evaluation for sustainable development of Himalayan agriculture using RS-GIS in conjunction with analytic hierarchy process and frequency ratio. *J. Saudi Soc. Agric. Sci.* **2021**, *20*, 1–17. [CrossRef]
7. Kordrostami, F.; Attarod, P.; Abbaspour, K.C.; Ludwig, R.; Etemad, V.; Alilou, H.; Bozorg-Haddad, O. Identification of optimum afforestation areas considering sustainable management of natural resources, using geo-environmental criteria. *Ecol. Eng.* **2021**, *168*, 106259. [CrossRef]
8. Prefectura Bolívar. Plan de Desarrollo y Ordenamiento Territorial de la Provincia Bolívar 2015–2020. Available online: https://bolivar.gob.ec/ (accessed on 9 May 2024).
9. Ahmed, I.; Das (Pan), N.; Debnath, J.; Bhowmik, M.; Bhattacharjee, S. Flood hazard zonation using GIS-based multi-parametric Analytical Hierarchy Process. *Geosyst. Geoenviron.* **2024**, *3*, 100250. [CrossRef]
10. Burayu, D.G.; Karuppannan, S.; Shuniye, G. Identifying flood vulnerable and risk areas using the integration of analytical hierarchy process (AHP), GIS, and remote sensing: A case study of southern Oromia region. *Urban Climb.* **2023**, *51*, 101640. [CrossRef]
11. Ally, A.M.; Yan, J.; Bennett, G.; Lyimo, N.N.; Mayunga, S.D. Assessment of groundwater potential zones using remote sensing and GIS-based fuzzy analytical hierarchy process (F-AHP) in Mpwapwa District, Dodoma, Tanzania. *Geosyst. Geoenviron.* **2024**, *3*, 100232. [CrossRef]
12. Malczewski, J. GIS-Based Multicriteria Decision Analysis: A Survey of the Literature. *Int. J. Geogr. Inf. Sci.* **2006**, *20*, 703–726. [CrossRef]
13. Ennaji, W.; Barakat, A.; Karaoui, I.; El Baghdadi, M.; Arioua, A. Remote sensing approach to assess salt-affected soils in the north-east part of Tadla plain, Morocco. *Geol. Ecol. Landsc.* **2018**, *2*, 22–28. [CrossRef]
14. Mallick, S.K.; Rudra, S. Analysis of Groundwater Potentiality Zones of Siliguri Urban Agglomeration Using GIS-Based Fuzzy-AHP Approach. In *Groundwater and Society: Applications of Geospatial Technology*; Shit, P.K., Bhunia, G.S., Adhikary, P.P., Dash, C.J., Eds.; Springer International Publishing: Cham, Switzerland, 2021; pp. 141–160; ISBN 978-3-030-64136-8.
15. Worqlul, A.W.; Haddad, M.; Alemayehu, S.; Govind, A. Developing a satellite-based combined land degradation index for monitoring environmental change: A case study in Tana-Beles watershed, Upper Blue Nile, Ethiopia. *Remote Sens. Appl.* **2023**, *32*, 101050. [CrossRef]
16. Senanayake, S.; Pradhan, B.; Huete, A.; Brennan, J. Proposing an ecologically viable and economically sound farming system using a matrix-based geo-informatics approach. *Sci. Total Environ.* **2021**, *794*, 148788. [CrossRef] [PubMed]
17. Olsson, L.; Barbosa, H.; Bhadwal, S.; Cowie, A.; Delusca, K.; Flores-Renteria, D.; Hermans, K.; Jobbagy, E.; Kurz, W.; Li, D.; et al. Land Degradation: IPCC Special Report on Climate Change, Desertification. In *IPCC Special Report on Climate Change, Desertification, Land Degradation*; Intergovernamental Panel on Climate Change (IPCC): Geneva, Switzerland, 2019; p. 1.
18. UNCCD. Convención Internacional de Lucha Contra la Desertificación en Los Países Afectados por Sequía Grave o Desertificación en Particular en África | Observatorio del Principio 10. Available online: https://observatoriop10.cepal.org/es/tratado/convencion-internacional-lucha-la-desertificacion-paises-afectados-sequia-grave-o (accessed on 18 December 2023).
19. Pimentel, D.; Kounang, N. Ecology of Soil Erosion in Ecosystems. *Ecosystems* **1998**, *1*, 416–426. [CrossRef]

20. MAG. Ministerio de Agricultura y Ganadería del Ecuador, (MAG). Available online: https://www.agricultura.gob.ec/ (accessed on 18 December 2023).
21. Montgomery, D.R. Soil erosion and agricultural sustainability. *Proc. Natl. Acad. Sci. USA* **2007**, *104*, 13268–13272. [CrossRef] [PubMed]
22. García-Ruiz, J.M.; Beguería, S.; Nadal-Romero, E.; González-Hidalgo, J.C.; Lana-Renault, N.; Sanjuán, Y. A meta-analysis of soil erosion rates across the world. *Geomorphology* **2015**, *239*, 160–173. [CrossRef]
23. Fick, S.E.; Hijmans, R.J. WorldClim 2: New 1-km spatial resolution climate surfaces for global land areas. *Int. J. Climatol.* **2017**, *37*, 4302–4315. [CrossRef]
24. Rachel, C. Dulcepamba Environmental Analysis. Bachelor's Thesis, Latin American Environment and Society, Pitzer College, Clermont, CA, USA, 2016.
25. IGM. Instituto Geográfico Militar, Cartografía de Libre Acceso. Available online: https://www.geoportaligm.gob.ec/portal/index.php/descargas/cartografia-de-libre-acceso/ (accessed on 4 February 2024).
26. Newmiller, J.; Walker, W.; Fleenor, W.E.; Pinter, N. Case Study: Reconstructing the 2015 Dulcepamba River Flood Disaster. *Environ. Eng. Geosci.* **2020**, *26*, 393–404. [CrossRef]
27. Copernicus. Copernicus Data Space Ecosystem | Europe's Eyes on Earth. Available online: https://dataspace.copernicus.eu/ (accessed on 18 June 2023).
28. Bachri, S.; Sumarmi, S.; Irawan, L.; Utaya, S.; Nurdiansyah, F.; Nurjanah, A.; Tyas, L.; Adillah, A.; Purnama, D. Landslide Susceptibility Mapping (LSM) in Kelud Volcano Using Spatial Multi-Criteria Evaluation. *IOP Conf. Ser. Earth Environ. Sci.* **2019**, *273*, 012014. [CrossRef]
29. Mattivi, P.; Franci, F.; Lambertini, A.; Bitelli, G. TWI computation: A comparison of different open source GISs. *Open Geospat. Data Softw. Stand.* **2019**, *4*, 6. [CrossRef]
30. Riley, S.; Degloria, S.; Elliot, S.D. A Terrain Ruggedness Index that Quantifies Topographic Heterogeneity. *Int. J. Sci.* **1999**, *5*, 23–27.
31. Esri Focal Statistics (Spatial Analyst)—ArcGIS Pro | Documentation. Available online: https://pro.arcgis.com/en/pro-app/latest/tool-reference/spatial-analyst/focal-statistics.htm (accessed on 10 July 2023).
32. Bannari, A.; Ghadeer, A.; El-Battay, A.; Hameed, N.A.; Rouai, M. *Detection of Areas Associated with Flash Floods and Erosion Caused by Rainfall Storm Using Topographic Attributes, Hydrologic Indices, and GIS*; Pirasteh, S., Li, J., Eds.; Springer International Publishing: Berlin/Heidelberg, Germany, 2017; pp. 155–174.
33. Aparicio, F. *Fundamentos de Hidrología de Superficie*; Limusa: Ciudad de México, Mexico, 1999; ISBN 968-18-3014-8.
34. Sinshaw, B.G.; Belete, A.M.; Tefera, A.K.; Dessie, A.B.; Bizuneh, B.B.; Alem, H.T.; Atanaw, S.B.; Eshete, D.G.; Wubetu, T.G.; Atinkut, H.B.; et al. Prioritization of potential soil erosion susceptibility region using fuzzy logic and analytical hierarchy process, upper Blue Nile Basin, Ethiopia. *Water Energy Nexus* **2021**, *4*, 10–24. [CrossRef]
35. Jenks, G.F.; Caspall, F.C. Error on Choroplethic Maps: Definition, Measurement, Reduction. *Ann. Assoc. Am. Geogr.* **1971**, *61*, 217–244. [CrossRef]
36. Wind, Y.; Saaty, T. Marketing applicatons of the analytic hierarchy process. *Manag. Sci.* **1980**, *26*, 641–658. [CrossRef]
37. Kayastha, P.; Dhital, M.R.; De Smedt, F. Application of the analytical hierarchy process (AHP) for landslide susceptibility mapping: A case study from the Tinau watershed, west Nepal. *Comput. Geosci.* **2013**, *52*, 398–408. [CrossRef]
38. Saaty, T. Relative Measurement and Its Generalization in Decision Making Why Pirwise Comparisons are Central in Mathematics for the Measurement of Intangible Factors the Analytic Hierarchy/Network Process. *Stat. Oper. Res.* **2008**, *102*, 251–318.
39. Saaty, T.L.; Vargas, L.G. *Decision Making with the Analytic Network Process*, 2nd ed.; Springer: Berlin/Heidelberg, Germany, 2006; ISBN 978-1-4614-7279-7.
40. Saaty, T.L.; Vargas, L.G. The possibility of group choice: Pairwise comparisons and merging functions. *Soc. Choice Welf.* **2012**, *38*, 481–496. [CrossRef]
41. Saaty, T.L.; Vargas, L.G. *Decision Making with the Analytic Network Process*; Springer: Berlin/Heidelberg, Germany, 2013; Volume 195. [CrossRef]
42. Budescu, D.V.; Swick, R.; Amnon, R. A comparison of the eigenvalue method and the geometric mean procedure for ratio scaling. *Appl. Psychol. Meas.* **1986**, *10*, 69–78. [CrossRef]
43. Sánchez, E. Evaluación multicriterio de la vulnerabilidad biofísica ante inundaciones de la cuenca del río Atacames-Esmeraldas-Ecuador. In *Sensores Remotos, GIS y Software R, Aplicado a Hidrogeología y Cambio Climático*; Centro de Publicaciones PUCE: Quito, Ecuador, 2021; pp. 33–56; ISBN 978-9978-77-625-4.
44. Arabameri, A.; Pradhan, B.; Pourghasemi, H.R.; Rezaei, K. Identification of erosion-prone areas using different multi-criteria decision-making techniques and gis. *Geomat. Nat. Hazards Risk* **2018**, *9*, 1129–1155. [CrossRef]
45. Lawal, D.U.; Matori, A.N.; Yusof, K.W.; Hashim, A.M.; Aminu, M.; Sabri, S.; Balogun, A.L.; Chandio, I.A.; Mokhtar, M.R.M. group-based decision support for flood hazard forecasting: A geospatial technology-based group analytic hierarchy process approach. *Res. J. Appl. Sci. Eng. Technol.* **2014**, *7*, 4838–4850. [CrossRef]
46. Sarkar, S.K.; Rudra, R.R.; Nur, M.S.; Das, P.C. Partial least-squares regression for soil salinity mapping in Bangladesh. *Ecol. Indic.* **2023**, *154*, 110825. [CrossRef]
47. Liu, Y.; Li, T.; Zhao, W.; Wang, S.; Fu, B. Landscape functional zoning at a county level based on ecosystem services bundle: Methods comparison and management indication. *J. Environ. Manag.* **2019**, *249*, 109315. [CrossRef]

48. Bai, Z.; Han, L.; Jiang, X.; Liu, M.; Li, L.; Liu, H.; Lu, J. Spatiotemporal evolution of desertification based on integrated remote sensing indices in Duolun County, Inner Mongolia. *Ecol. Inform.* **2022**, *70*, 101750. [CrossRef]
49. Moore, I.D.; Grayson, R.B.; Ladson, A.R. Digital terrain modelling: A review of hydrological, geomorphological, and biological applications. *Hydrol. Process.* **1991**, *5*, 3–30. [CrossRef]
50. Moore, I.D.; Turner, A.K.; Wilson, J.P.; Jenson, S.K.; Band, L.E. GIS and Land-Surface-Surface Process Modeling. In *Environmental Modeling with GIS*; Oxford University: Oxford, UK, 1993.
51. Alilou, H.; Rahmati, O.; Singh, V.; Choubin, B.; Pradham, B.; Keesstra, S.; Ghiasi, S.; Sageghi, S. Evaluation of watershed health using Fuzzy-ANP approach considering geo-environmental and topo-hydrological criteria. *J. Environ. Manag.* **2019**, *232*, 22–36. [CrossRef]
52. Florinsky, I.V.; Eilers, R.G.; Manning, G.R.; Fuller, L.G. Prediction of soil properties by digital terrain modelling. *Environ. Model. Softw.* **2002**, *17*, 295–311. [CrossRef]
53. Beven, K.J.; Kirkby, M.J. A physically based, variable contributing area model of basin hydrology/Un modèle à base physique de zone d'appel variable de l'hydrologie du bassin versant. *Hydrol. Sci. Bull.* **1979**, *24*, 43–69. [CrossRef]
54. Schmidt, F.; Persson, A. Comparison of DEM data capture and topographic wetness indices. *Precis. Agric.* **2003**, *4*, 179–192. [CrossRef]
55. Thakkar, A.K.; Dhiman, S.D. Morphometric analysis and prioritization of miniwatersheds in Mohr watershed, Gujarat using remote sensing and GIS techniques. *J. Indian Soc. Remote Sens.* **2007**, *35*, 313–321. [CrossRef]
56. Aher, P.D.; Adinarayana, J.; Gorantiwar, S.D. Quantification of morphometric characterization and prioritization for management planning in semi-arid tropics of India: A remote sensing and GIS approach. *J. Hydrol.* **2014**, *511*, 850–860. [CrossRef]
57. Fukuyama, T.; Onda, Y.; Takenata, C.; Walling, D. Investigating erosion rates within a Japanese cypress plantation using Cs-137 and Pb-210ex measurements. *J. Geophys. Res.* **2008**, *113*, F2. [CrossRef]
58. Mirzai, M.; Sajadi, A.; Nazari, A. Modeling and simulation of watershed erosion: Case study of Latian dam watershed. *Int. J. Phys. Sci.* **2014**, *9*, 224–232. [CrossRef]
59. Vermeulen, S.J.; Aggarwal, P.K.; Ainslie, A.; Angelone, C.; Campbell, B.M.; Challinor, A.J.; Hansen, J.W.; Ingram, J.S.I.; Jarvis, A.; Kristjanson, P.; et al. Options for support to agriculture and food security under climate change. *Environ. Sci. Policy* **2012**, *15*, 136–144. [CrossRef]
60. Wollenberg, E.; Vermeulen, S.J.; Girvetz, E.; Loboguerrero, A.M.; Ramirez-Villegas, J. Reducing risks to food security from climate change. *Glob. Food Secur.* **2016**, *11*, 34–43. [CrossRef]
61. Elsheikh, R.; Mohamed Shariff, A.R.B.; Amiri, F.; Ahmad, N.B.; Balasundram, S.K.; Soom, M.A.M. Agriculture Land Suitability Evaluator (ALSE): A decision and planning support tool for tropical and subtropical crops. *Comput. Electron. Agric.* **2013**, *93*, 98–110. [CrossRef]
62. Montgomery, B.; Dragićević, S.; Dujmović, J.; Schmidt, M. A GIS-based Logic Scoring of Preference method for evaluation of land capability and suitability for agriculture. *Comput. Electron. Agric.* **2016**, *124*, 340–353. [CrossRef]
63. Cherlet, M.; Hill, J.; Von Maltitz, G.; Sommer, S.; Reynolds, J.; Hutchinson, C.; Cherlet, M. *World Atlas of Desertification: Rethinking Land Degradation and Sustainable Land Management*; Publications Office of the European Union: Luxembourg, 2018; ISBN 978-92-79-75349-7.
64. Foley, J.A.; Ramankutty, N.; Brauman, K.A.; Cassidy, E.S.; Gerber, J.S.; Johnston, M.; Mueller, N.D.; O'Connell, C.; Ray, D.K.; West, P.C.; et al. Solutions for a cultivated planet. *Nature* **2011**, *478*, 337–342. [CrossRef] [PubMed]
65. Foley, J.A.; DeFries, R.; Asner, G.P.; Barford, C.; Bonan, G.; Carpenter, S.R.; Chapin, F.S.; Coe, M.T.; Daily, G.C.; Gibbs, H.K.; et al. Global Consequences of Land Use. *Science* **2005**, *309*, 570–574. [CrossRef] [PubMed]
66. Gibbs, H.K.; Salmon, J.M. Mapping the world's degraded lands. *Appl. Geogr.* **2015**, *57*, 12–21. [CrossRef]
67. Bai, Z.G.; Dent, D.L.; Olsson, L.; Tengberg, A.; Tucker, C.; Yengoh, G. A longer, closer, look at land degradation. *Agric. Dev.* **2015**, *24*, 3–9.
68. Schut, A.G.T.; Ivits, E.; Conijn, J.G.; Brink, B.T.; Fensholt, R. Trends in Global Vegetation Activity and Climatic Drivers Indicate a Decoupled Response to Climate Change. *PLoS ONE* **2015**, *10*, e0138013. [CrossRef]
69. Middleton, N.; Thomas, D. *World Atlas of Desertification*, 2nd ed.; Edward Arnold: Sevenoaks, UK, 1997; ISBN 978-0-340-69166-3.
70. Jain, S.K.; Goel, M.K. Assessing the vulnerability to soil erosion of the Ukai Dam catchments using remote sensing and GIS. *Hydrol. Sci. J.* **2002**, *47*, 31–40. [CrossRef]
71. Mysiak, J.; Giupponi, C.; Rosato, P. Towards the development of a decision support system for water resource management. *Environ. Model. Softw.* **2005**, *20*, 203–214. [CrossRef]
72. Rahman, M.R.; Shi, Z.H.; Chongfa, C. Assessing regional environmental quality by integrated use of remote sensing, GIS, and spatial multi-criteria evaluation for prioritization of environmental restoration. *Environ. Monit. Assess.* **2014**, *186*, 6993–7009. [CrossRef]
73. Shao, Z.; Huq, M.E.; Cai, B.; Altan, O.; Li, Y. Integrated remote sensing and GIS approach using Fuzzy-AHP to delineate and identify groundwater potential zones in semi-arid Shanxi Province, China. *Environ. Model. Softw.* **2020**, *134*, 104868. [CrossRef]
74. Ghosh, A.; Maiti, R. Development of new Ecological Susceptibility Index (ESI) for monitoring ecological risk of river corridor using F-AHP and AHP and its application on the Mayurakshi river of Eastern India. *Ecol. Inform.* **2021**, *63*, 101318. [CrossRef]
75. Conrad, R. Proyecto Dulcepamba. Available online: https://www.proyectodulcepamba.org (accessed on 11 May 2024).

76. Jiang, C.; Yang, Z.; Liu, C.; Dong, X.; Wang, X.; Zhuang, C.; Zhao, L. Win-win-win pathway for ecological restoration by balancing hydrological, ecological, and agricultural dimensions: Contrasting lessons from highly eroded agroforestry. *Sci. Total Environ.* **2021**, *774*, 145140. [CrossRef]
77. Knighton, L.N.; Petersen, S.L.; Collins, G.H.; Allphin, L.; Hansen, N.C.; Johnston, H.B.; Rader, R.B. Hydrologic restoration of anthropoentically altered springs in the Sheldon National Wildlife Refuge in the Great Basin, USA. *J. Arid. Environ.* **2023**, *211*, 104944. [CrossRef]
78. Albarracín, M.; Ramón, G.; González, J.; Iñiguez-Armijos, C.; Zakaluk, T.; Martos-Rosillo, S. The Ecohydrological Approach in Water Sowing and Harvesting Systems: The Case of the Paltas Catacocha Ecohydrology Demonstration Site, Ecuador. *Ecohydrol. Hydrobiol.* **2021**, *21*, 454–466. [CrossRef]
79. Zalewski, M.; Kiedrzyńska, E.; Wagner, I.; Izydorczyk, K.; Boczek, J.M.; Jurczak, T.; Krauze, K.; Frankiewicz, P.; Godlewska, M.; Wojtal-Frankiewicz, A.; et al. Ecohydrology and adaptation to global change. *Ecohydrol. Hydrobiol.* **2021**, *21*, 393–410. [CrossRef]
80. Yang, Z.; Dai, X.; Lu, H.; Liu, C.; Nie, R.; Zhang, M.; Ma, L.; Li, N.; Liu, T.; He, Y.; et al. Evaluation and prediction of water conservation of the Yellow river basin in Sichuan Province, China, based on Google Earth Engine and CA-Markov. *Heliyon* **2023**, *9*, e17903. [CrossRef] [PubMed]